ANNALS OF GEOPHYSICS, 68, 3, NS339, 2025; doi:10.4401/ag-9249
OPEN ACCESS

Use of *in situ* tests to measure and predict shear wave velocity: the peculiarity of silty-sandy deposits in Emilia (Italy)

Christian Valvano[*,1], Sara Amoroso[1,2], Salomon Hailemikael[2], Luca Minarelli[2], Kyle M. Rollins[3]

(1) University of Chieti-Pescara, Pescara, Italy
(2) Istituto Nazionale di Geofisica e Vulcanologia, Roma, Italy
(3) Brigham Young University, Provo, Utah

Article history: received January 15, 2025; accepted June 9, 2025

Abstract

The results of Medusa SDMT (Seismic Dilatometer) and SCPTu (Seismic Piezocone) that were performed in 2023 at two different sites in the Emilia (Italy) plain are described in this paper. The focus is on the measurement of the shear wave velocity (V_s) and the predictive capability of existing (cone penetration test – CPT and flat dilatometer – DMT based) empirical correlations. Both the pseudo-interval and true interval approaches were applied when interpreting the *in situ* measurements. The comparison between measured V_s (SDMT – true interval) and predicted V_s from four different CPT and one DMT empirical correlations shows that not all of them have good performance. In this respect, we propose an updated DMT correlation to improve the accuracy of the predicted V_s in silty-sandy deposits, which are predominant in the sites investigated in this paper. The studies connected to these peculiar intermediate soils are still ongoing and their behavior needs further research sites to test and validate this preliminary correlation.

Keywords: Shear wave velocity; Medusa seismic dilatometer; Seismic piezocone; Silty-sandy deposits; Geotechnical and geophysical data

1. Introduction

The European Building Code (CEN, 2004), as well as several national building codes, gives indications about the importance of evaluating the shear wave velocity (V_s) profile when the soil characterization needs to be defined. This code implements a seismic subsoil classification based on the value of the equivalent shear wave velocity ($V_{s,eq}$), calculated as a function of the different homogeneous V_s layers detected within the upper 30 m of subsoil or less, which is considered a proxy for ground-motion amplification caused by earthquakes (Borcherdt, 1994, among many others).

The V_s can be measured with invasive or non-invasive geophysical methods. Invasive methods advance equipment into the ground and can generally be divided into cross-hole (CH) and down-hole (DH) methods

(e.g. Zhou et al., 2023). CH tests advance both the seismic source and receiver(s) to various measurement depths into different boreholes while DH soundings use a seismic source at the ground surface and advance receiver(s) to various measurement depths. The cross-hole test (CH) is considered the most reliable invasive method, as the measurements are performed locally at any specific depth along short travel paths (Garofalo et al., 2016). The V_s derived from CH and DH methods are influenced by the properties of the volume of soil between the source and receiver(s) and the polarity of the generated shear waves. They can be horizontally (SH) or vertically polarized (SV) and if the geophones are horizontal, it is important to generate only pure SH waves. If they are mixed with SV waves, the receiver will record an altered signal and it could result in misinterpretation of the V_s profile. Triaxial geophones can more easily identify SH waves, improving the definition of the V_s profile. The way through which the energization of the seismic source is done and the reciprocal orientation of the geophones and seismic source axis are important factors affecting the generation of pure SH waves and their recognition (ASTM D7400/D7400M-19, 2019). About the influence of the properties of the volume of soil between the source and receivers, Foti et al. (2006) remarked how the shear wave velocity is a function of the shear modulus in the horizontal plane, G_{HH}, and the shear modulus in the vertical plane, G_{VH}, which are different because of the intrinsic anisotropy of the soil. DH methods, which consider slanted ray path of seismic waves, are influenced by both G_{HH} and G_{VH}. Foti et al. (2006) demonstrated that varying the distance between the hole and the seismic source, hence the direction of propagation of waves, the values of G_{HH} and G_{VH} could be obtained. If the medium between the receivers is assumed to be isotropic, the velocities measured with different distances should coincide, but it is observed that it is not the case and the differences can be interpreted with an anisotropic model.

Non-invasive methods are based on measurements performed along the ground surface, and consequently their main advantage is that the sources and receivers do not need to penetrate the ground. Non-invasive methods include seismic refraction, seismic reflection, and surface wave methods (e.g. Stacul et al., 2024). The seismic refraction method is based on the principle that when a seismic wave reaches a boundary across which there is a contrast in velocity, then the direction of travel of that wave changes upon entry into the new material. The waves produced on surface travel in three principal ways: directly along the top of the ground surface (direct wave), by reflection from the top of the refractor, and by critical refraction along the top of the refractor(s). The arrival of each wave is detected along a set of geophones and recorded on a seismograph (Reynolds, 1997). The seismic reflection technique is set to measure the time taken for a seismic wave to travel from a source down into the ground where it is reflected back to the surface and then detected at a receiver, which measures the two-way travel time. This seismic method is used to obtain important details, not only about the geometry of different layers and to detect the depth of the bedrock, but also about the physical properties of the materials present (Reynolds, 1997). The surface wave method is the most popular non-invasive method because it is time and cost effective and it can be applied to a variety of ground conditions, but it is affected by non-uniqueness of the solution and this leads to interpretation ambiguities since several possible V_s profiles are solutions to the inverse problem (Garofalo et al., 2016).

With respect to invasive methods, there are some *in situ* probes (e.g. Cone penetration test CPT and dilatometer test DMT) that measure V_s but can also be used to define soil stratigraphy and geotechnical parameters (Mayne, 2006). Robertson (1986) provides a detailed overview of many of the standardized and specialized devices that are primarily penetration type and/or direct-insertion type devices for testing the ground. Woods (1978) and Campanella (1994) give a review of applicable geophysical tests for determining mechanical wave properties. An optimization of site-specific site investigation is achieved with seismic piezocone testing SCPTu (Campanella et al., 1986) and seismic dilatometer test SDMT (Hepton, 1988), which both adopt the DH-type approach and allow one to obtain both the V_s profile and many geotechnical parameters.

An important comparison shown in Foti et al. (2006) consists of V_s profiles obtained at Fucino Site (Italy) by SDMT, SCPT (both adopting DH approach), SASW (non-invasive method) and CH test: they are all in good agreement and this led to not consider anisotropy to have different influences on the results if DH or CH methods or non-invasive methods are adopted. Monaco et al. (2013) shows a wide collection of geotechnical *in situ* test results from the city of L'Aquila (Italy) and it can be seen that the V_s profiles obtained by SDMT are generally in acceptable agreement with the V_s profiles obtained with DH and CH testing, while the agreement with the V_s profiles obtained by MASW in some cases is less satisfactory. Stacul et al. (2024) presents some comparisons between four Italian different sites where seismic reflection tests, SCPTu, SDMT, and CH testing were implemented: also, this paper gives satisfactory results about this kind of comparison. A general agreement between DH and CH testing results is confirmed in literature (e.g. Roesler, 1979; Jamiolkowski et al., 1991; Lo Presti et al., 1991; Stokoe et al., 1991; Bellotti et al., 1996; Jamiolkowski et al., 1998; Lo Presti et al., 1999).

Two different interval methods can be undertaken to obtain V_s from seismograms recorded by receivers during the execution of a DH-type testing (Garofalo et al., 2016): the true-interval and the pseudo-interval. The true-interval implies the calculation of the time delay (Δt) in the onset of the same seismic wave by two geophones at different depths through a cross-correlation algorithm. The pseudo-interval approach considers the seismogram recorded at different depths separately, leading to two different analyses. Manual picking of the first arrival of the signal is carried out on seismograms at each acquisition depth.

As it is also stressed in Amoroso et al. (2016), the true-interval approach is better conditioned because it is based on a wide portion of the seismograms rather than on just the first arrival of the signal. The pseudo-interval approach is very sensitive to measurement errors (Garofalo et al., 2016): the difference between two subsequent first arrival is usually very small. Therefore, their identification could vary among different operators, resulting in magnification of the measurement error. Garofalo et al. (2016) shows also that the operations of manual picking could be more difficult if tube waves are recorded in the borehole.

When the S-wave direct measurements are challenging or the elaboration of a V_s profile is needed in a site where no direct geophysical testing has been executed, the estimation of V_s through the application of an empirical correlation could be very helpful. In recent decades, researchers have been prolific in developing correlations between V_s and non-seismic test results from the SPT, CPT and DMT (e.g. Bouchovalas et al., 1989; Baldi et al., 1989; Rix and Stokoe, 1991; Fear and Robertson, 1995; Hegazy and Mayne, 1995; Simonini and Cola, 2000; Madiai and Simoni, 2004; Mayne, 2006; Andrus et al., 2007; Marchetti et al., 2008; Robertson, 2009; Vera-Grunauer, 2014; McGann et al., 2015). In the absence of direct V_s measurements, this approach can be used, for example, in seismic ground response studies conducted in environments where liquefaction could happen, such as alluvial plains. However, the *in situ* direct measurements are more accurate than the estimations coming from these empirical relationships, because they are strictly dependent on site characteristics, such as geological age, stress history, effective stress state, soil material type, cementation, and consolidation. In this respect, it becomes difficult to obtain a correlation that can account for all the afore-mentioned parameters between many different sites. Therefore, an empirical correlation should only be used when the soil of interest is well represented in the database underlying its development (e.g. Akin et al., 2011; Amoroso, 2014; Intriago et al., 2020; Zhou et al., 2023; Uzielli et al., 2024).

This paper illustrates an example of a practical application of SCPTu and SDMT testing in Emilia (Italy), an area subjected to a seismic sequence during May 2012, which caused widespread surficial liquefaction features (Minarelli et al., 2022). The *in situ* geotechnical test campaign was carried out in 2023 at two sites that liquefied in 2012 located in Mirandola (Province of Modena) and Bondeno (Province of Ferrara). The measured V_s profiles are compared with the predicted V_s values based on DMT (Marchetti et al., 2008) and CPT correlations (Hegazy and Mayne, 1995; Madiai and Simoni, 2004; Andrus et al., 2007). A modification to the Marchetti et al. (2008) relationship is discussed to improve the performance of the original empirical model, especially in materials that can be defined as silts, according to the material index (I_D) values.

2. Geological setting

A northeastern portion of the Emilia-Romagna region, Italy, was struck by an earthquake sequence in May 2012 (Pondrelli et al., 2012). The seismic sequence was characterized by two main shocks, followed by many aftershocks, generated by various compressional tectonic structures, part of the front of the Apennine chain buried under the Po alluvial plain (Fig. 1).

The strongest shock ($M_W = 6.1$) occurred on May 20th with epicenter near Finale Emilia, while the second largest earthquake ($M_W = 5.9$), took place on May 29th with epicenter close to Mirandola. The two main events generated widespread surficial liquefaction features, which mainly took place within buried fluvial channel sandy deposits of Holocene age (e.g. Civico et al., 2015; Minarelli et al., 2022).

Both epicenters and liquefaction sites are located south of the Po River and northwest of the Reno River, between the Secchia and Panaro Apennine rivers which are tributaries of the Po River (Fig. 1). These rivers changed courses through time, depositing thick late Pleistocene and Holocene successions, forming the shallow subsurface of the investigated alluvial plain area (Minarelli et al., 2022).

In the study area, the subsurface consists of extensive deposits of medium to coarse sand, sedimented during the Upper Pleistocene by the Po into braided river environments, overlain by interfluvial fine-grained sediments, interspersed with river sand bodies, often deposited into meandering channels. These channels often reworked

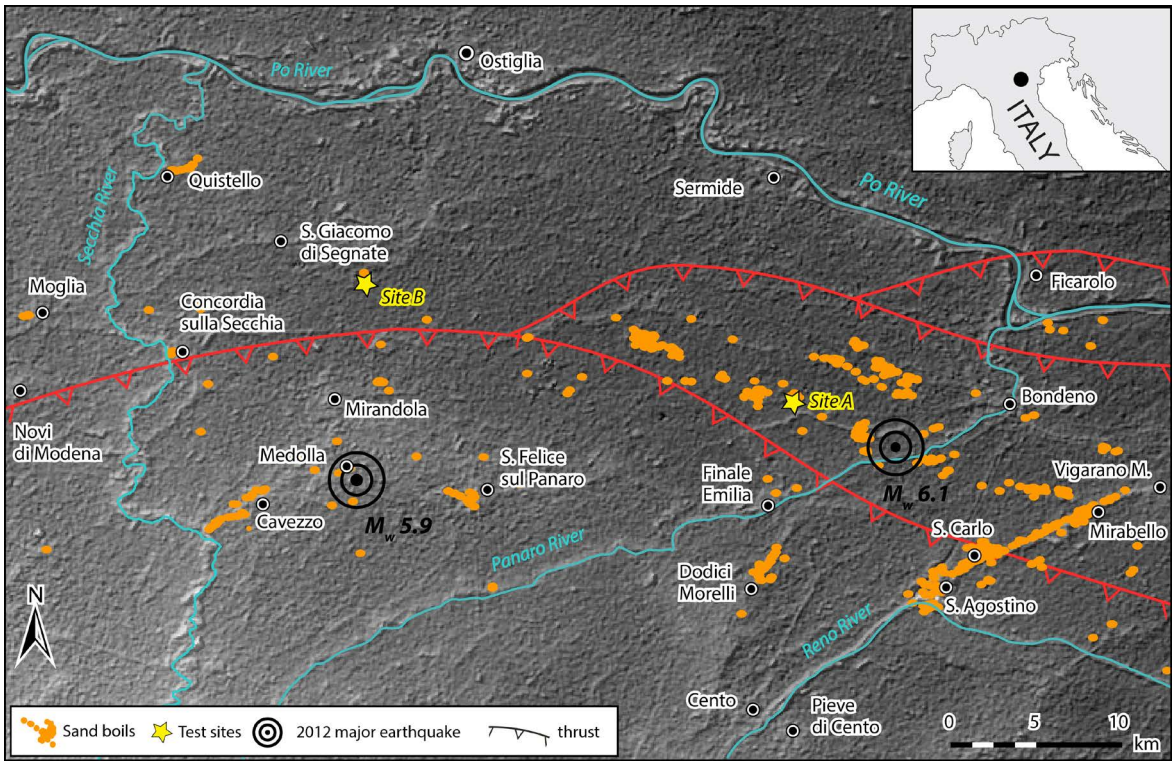

Figure 1. The map shows the portion of the Emilia-Romagna Region affected by the seismic sequence of May 2012 and the distribution of coseismic liquefaction observations. The buried thrust structures that caused the two mainshocks are shown with their epicenters. Orange dots are the sand boils that erupted at the surface. Site A and Site B (yellow stars) indicate the location of tests analyzed in this paper.

Upper Pleistocene deposits, generating thick continuous successions of sands. Southward, the Po River deposits grade into mainly clayey and silty sediments provided by the Apennine rivers (Minarelli et al., 2022).

During the last decade several studies have been performed to improve the geological knowledge of the subsurface (e.g. Stefani et al., 2018; Bruno et al., 2021; Demurtas et al., 2024), and to investigate the geotechnical properties of the deposits subject to the liquefaction phenomena using *in situ* tests (e.g. Facciorusso et al., 2015; Tonni et al., 2015; Minarelli et al., 2022) and full-scale induced liquefaction experiments (e.g. Amoroso et al., 2017; Flora et al., 2021; Amoroso et al., 2020).

3. Methods

3.1 Use of invasive methods for seismic site characterization

This study presents the results of the seismic piezocone (SCPTu) and Medusa seismic dilatometer (Medusa SDMT) tests performed at two research sites affected by liquefaction in 2012: Site A is located in the Bondeno Municipality (Scortichino village, Province of Ferrara) and Site B in the Mirandola Municipality (Tramuschio village, Province of Modena), as shown in Fig. 1. The investigation of these sites was part of a wider SCPTu-Medusa SDMT campaign, performed in 2023, within the USGS FY2022 EHP Program "Evaluation and Improvement of Methods to Consider Influence of Surface Clay Layers on Liquefaction-Induced Settlement from Large Database", coordinated by the Brigham Young University (Provo, Utah, USA) in collaboration with the Istituto Nazionale di Geofisica e Vulcanologia (Italy) and the University of Chieti-Pescara (Italy). The USGS project was aimed at understanding the features of the non-liquefiable crusts for improving prediction of ejecta features. In contrast, this study is focused on the comparison of measured V_s velocity profiles with those derived from available empirical methods for estimating V_s.

Figure 2 shows the geotechnical equipment that was used in Mirandola and Bondeno to measure the shear wave velocity (V_s): the Medusa seismic dilatometer (Medusa SDMT in Fig. 2a) and the seismic piezocone (SCPTu in Fig. 2b).

3.1.1 Medusa seismic dilatometer test

The Medusa SDMT (Marchetti, 2018; Marchetti et al., 2019) is a recent evolution of the seismic dilatometer (SDMT), with hydraulic automation and measuring system for autonomously performing DMT tests. This new equipment does no longer use the pneumatic cable, the control unit and the gas tank required in the traditional pneumatic DMT (ASTM D6635-01, 2017). A rechargeable battery pack powers an electronic board, connected to a pressure transducer and to a custom-designed motorized syringe, which hydraulically expands the membrane to obtain the DMT A, B and C pressure readings. The readings are stored automatically at each test depth (typically every 0.20 m). The Medusa SDMT incorporates additional sensors and components for the measurement of the shear wave velocity (Marchetti et al., 2008).

The seismic module (Fig. 2a) is placed above the DMT blade and it is equipped with two horizontal geophones spaced at 0.5 m vertically. The instrument progressively penetrates the soil and at both sites described in this paper, the penetration stopped every meter and the V_s value was measured. The energization of the seismic source is produced by a hammer blow (the one used during the cited campaign has a weight of 1.5 kg), which strikes a metallic plate, fixed on the ground and oriented with the longitudinal axis parallel to the axis of the receivers, to offer maximum sensitivity to the generated shear wave (S-wave horizontally polarized, SH). The metallic plate used during the geotechnical campaign was placed 2 m from the point where the Medusa SDMT was penetrating. The test was performed at standard penetration rate (20 mm/s) and at standard pressurization rate (i.e. first and second DMT pressure readings, A and B respectively, taken at about 15 s).

3.1.2 Seismic piezocone test

In the cone penetration test (CPT) the cone is pushed into the ground at a constant rate equal to 20 mm/s by means of a series of rods. During the penetration, electrical transducers send a signal to the control unit,

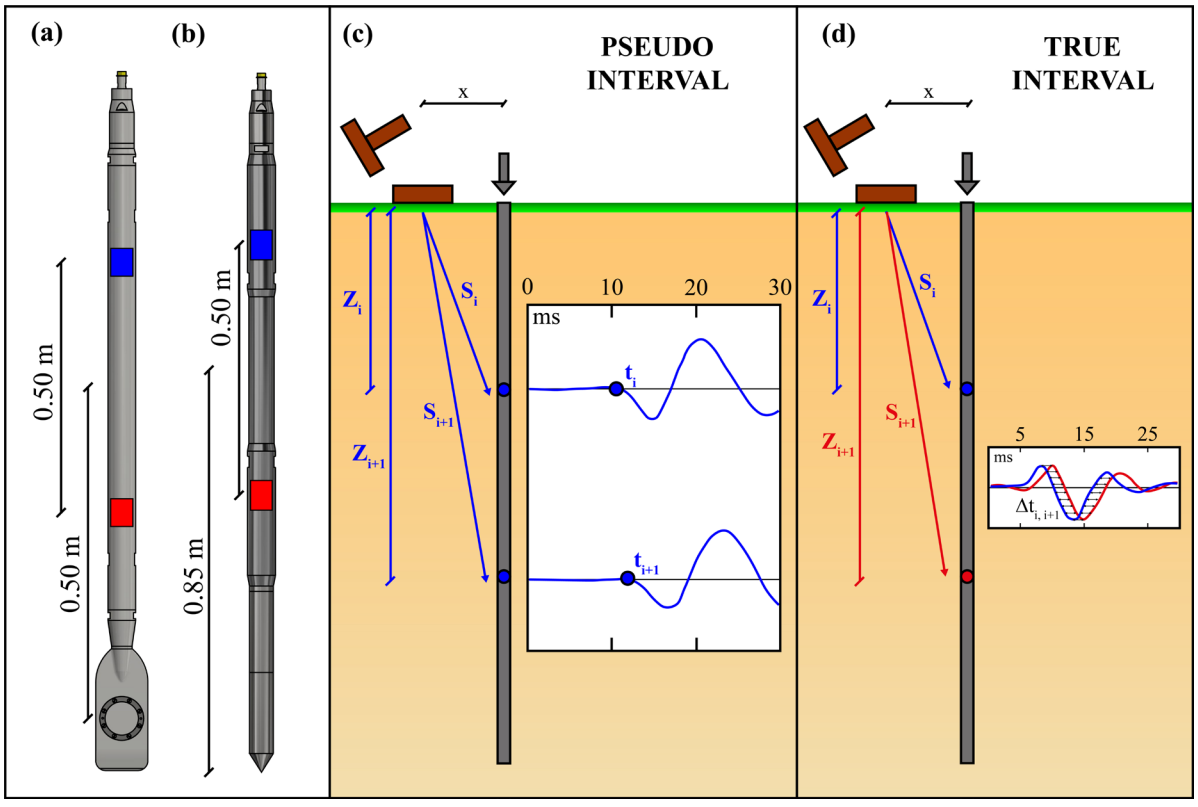

Figure 2. Layout of Medusa SDMT (a) and seismic piezocone (b) equipment: the locations of the geophones are highlighted with blue and red squares. A simplified outline of the S-wave interpretation is also reported using the pseudo-interval (c) and true-interval (d) approaches.

providing measurements of the cone tip resistance (q_C) and sleeve friction (f_S), typically acquired every 1-2 cm and plotted during the test on a screen. The term "piezocone" (CPTu) is used when the conical tip is paired with a porous element at its base called a filter, which also measures and records the interstitial pore water pressure (u_2), both during the advance and at the stationary position of the piezocone, in this latter case with dissipation tests (ASTM D5778-12, 2020).

A further evolution of the piezocone is the seismic piezocone (SCPTu), which is also able to acquire data on the shear wave velocity V_s, recording seismograms with geophones. The instrument used during the survey campaign (Fig. 2b) has two triaxial geophones spaced 0.50 m (blue and red squares). The shear waves were generated at the surface using a 1.5 kg hammer impacting on both sides of a metal plate, vertically embedded in the ground at a distance of 2 m from the SCPTu point of penetration. However, recent studies on SCPTu (Lo Presti et al., 2024) have suggested to fix the seismic source at a distance greater than 3 m from the rods. The impact for the S energization was carried out at every meter of depth into the soil, after blocking the pressure exerted on the rod battery, and it was repeated twice at each depth of investigation, hitting both on the left and right side of the metal plate. A straight-line travel path is commonly assumed from the source to receiver. The penetration rate adopted during the execution of the testing was 20 mm/s.

3.1.3 Determination of S-wave velocity

The seismograms of shear waves obtained from SCPTu and Medusa SDMT tests were processed to obtain V_s profiles. This was done by following the pseudo-interval and true-interval approaches; the former considers the arrival times of the signals generated by multiple sources and recorded by a single receiver at multiple depths while the latter considers the delay in the arrival times of the signals generated by the same source and recorded by a pair of receivers at different depths (ASTM D7400/D7400M-19, 2019).

With the pseudo-interval approach (Fig. 2c), the two geophones are considered separately, obtaining independent V_s profiles. The distance between the seismic source and the rods is x in Fig. 2c. In this case, a single impact source at the surface generates a single seismogram recorded by the geophone located at depth Z.

For each geophone, the first arrival (t_i) on the seismogram recorded at the i-th survey depth (Z_i) is recorded by manual picking (Fig. 2c). The $V_{s\ i,i+1}$ is the shear wave velocity associated with the depth range between Z_i and Z_{i+1}, and it is calculated as the ratio between the difference in source-receiver distances ($\Delta S_{i,i+1} = S_{i+1} - S_i$, see Fig. 2c) and the difference between the first arrival times ($\Delta t_{i,i+1} = t_{i+1} - t_i$, see Fig. 2c) recorded at the two consecutive survey depths (Eq. 1).

Using the true-interval approach, both geophones in each instrument are considered simultaneously, resulting in a single V_s profile (Fig. 2d). The seismic wave generated after the impact of the seismic source at the surface is recorded by both geophones, firstly by the upper one (blue) and then, after a certain time delay ($\Delta t_{i,i+1}$), also by the lower one (red). Each impact produces two seismograms recorded at two different depths and a cross-correlation algorithm provides the difference in first arrival times, allowing for the determination of the shear wave velocity at each depth interval, by applying (Eq. 1). The $V_{s\ i,i+1}$ is calculated with the same formula (Eq. 1) but considering data obtained with a single energization.

$$V_{s\ i,i+1} = \frac{\Delta S_{i,i+1}}{\Delta t_{i,i+1}} \tag{1}$$

With respect to the pseudo-interval approach which may suffer of inaccuracies due to triggering time issues, the true-interval test configuration avoids possible inaccuracies in the determination of the "zero time" at the hammer impact. Moreover, the pair of seismograms recorded by the two receivers at a given test depth-interval (true-interval approach) corresponds to the same hammer blow and not to different blows in sequence, which are not necessarily identical. Hence, the repeatability of velocity measurements is considerably improved using the true-interval approach.

The Results section presents comparisons of V_s profiles obtained at the two research sites, using both Medusa SDMT and SCPTu equipment with pseudo-interval and true-interval S-wave interpretations.

3.2 Estimation of shear wave velocity from correlations with *in situ* tests

The measured V_s profiles, obtained with the Medusa SDMT and interpreted with true-interval approach, were selected to be compared with predicted V_s profiles, elaborated using empirical correlations based on flat dilatometer (DMT) and cone penetration (CPT) tests. This comparison is performed for verifying the applicability of these correlations in the area of study when no direct geophysical measurements are available, considering the variability associated with natural soil deposits (e.g. geological age, soil type, cementation, effective stress state).

Among the available empirical V_s correlations based on CPT data, this study considers the formulas from Hegazy and Mayne (1995), Andrus et al. (2007), and Madiai and Simoni (2004), this last developed in the Italian territory, while for the DMT only one empirical correlation is available from Marchetti et al. (2008). The next sections discuss these predictive models.

3.2.1 Flat dilatometer test

Marchetti et al. (2008) proposed an empirical relationship between the small-strain shear modulus (G_0) normalized by the constrained modulus (M_{DMT}, obtained from DMT intermediate parameters according to Marchetti, 1980), and the horizontal stress index (K_D, obtained from DMT measured parameters according to Marchetti, 1980). The correlations are different for clays (Eq. 2), silts (Eq. 3) and sands (Eq. 4) according to the values of the material index (I_D, obtained from DMT measured parameters according to Marchetti, 1980):

$$\frac{G_0}{M_{DMT}} = 26.177 \cdot K_D^{-1.0066} \qquad Clays: I_D \leq 0.6 \tag{2}$$

$$\frac{G_0}{M_{DMT}} = 15.686 \cdot K_D^{-0.921} \qquad Silts: 0.6 < I_D \leq 1.8 \tag{3}$$

$$\frac{G_0}{M_{DMT}} = 4.5613 \cdot K_D^{-0.7967} \qquad Sands: I_D > 1.8 \tag{4}$$

where G_0 and M_{DMT} need to be in the same unit of measure (e.g. both in kPa or both in MPa) and K_D is dimensionless.

The plot of G_0/M_{DMT} versus K_D (Marchetti et al., 2008) presented in Fig. 3 has been defined using G_0, M_{DMT}, I_D and K_D values at the same depth determined by SDMT at 34 different sites, in a wide array of soil types. Most of the sites are in Italy, but others are from Spain, Poland, Belgium and the USA. The dependency of the ratio G_0/M_{DMT} on soil type and stress history is highlighted in Fig. 3, where distinct trends are observed for different ranges of I_D.

Marchetti et al. (2008) proposed (Eq. 2,3,4) to estimate G_0, from which the shear wave velocity V_s can then be computed through the fundamental relationship of the theory of elasticity:

$$V_s = \sqrt{\frac{G_0}{\rho}} \tag{5}$$

where ρ is soil density, that can be obtained from the unit weight (γ) using DMT testing data (Marchetti and Crapps, 1981) in the absence of undisturbed samples along the entire vertical sounding of interest.

3.2.2 Cone penetration test

The three CPT-V_s empirical correlations selected for this study (Hegazy and Mayne, 1995; Madiai and Simoni, 2004; Andrus et al., 2007) are applicable for different soil types. In particular, Madiai and Simoni (2004) and

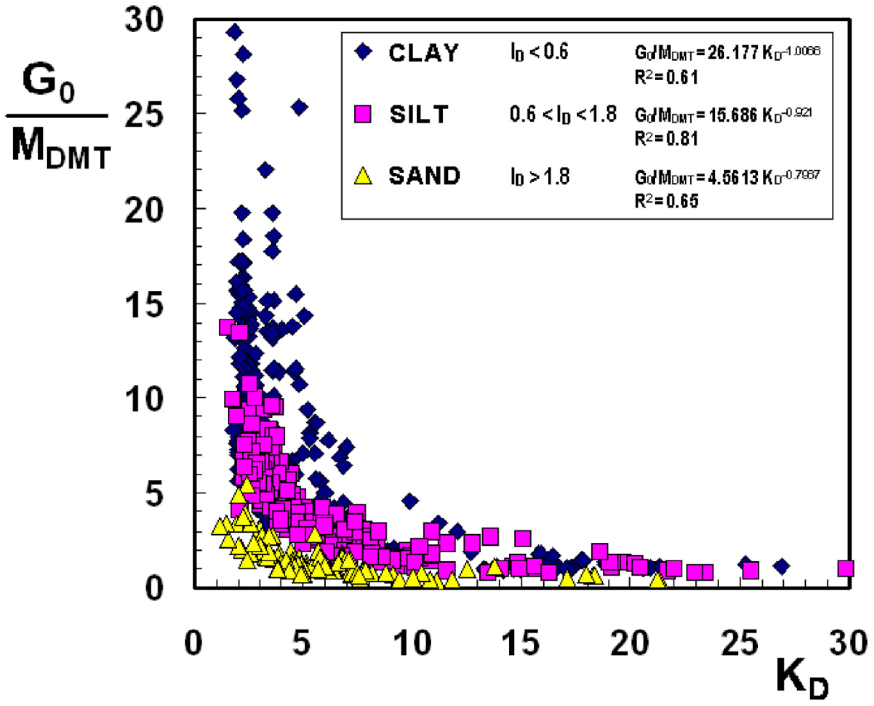

Figure 3. Empirical correlation between the ratio G_0/M_{DMT} and the horizontal stress index K_D using seismic dilatometer test data at 34 international research sites. The experimental points are grouped as a function of the material index I_D defining clay, silt, and sand (Figure from Marchetti et al., 2008).

Andrus et al. (2007) defined subcategories as a function of the geological age (Holocene for the soil deposits studied in Emilia area of study) and the soil type.

Hegazy and Mayne (1995) tried to improve the estimation of V_s in sand and clay soils and to develop a correlation independent of soil type. Their database is made up of 61 worldwide sites, representing different types of sands, clays, intermediate soils and mine tailings. The shear wave velocity data were measured using seismic cone, cross-hole, downhole and spectral analysis of surface waves and the equation for V_s in m/s is given by:

$$V_s = [10.1 \cdot \log(q_t) - 11.4]^{1.67} \cdot \left(\frac{f_s}{q_t} \cdot 100\right)^{0.3} \tag{6}$$

where q_t is the corrected cone resistance in kPa and f_s is the sleeve friction in kPa.

Andrus et al. (2007) defined a set of empirical equations for predicting V_s of soils of different geological age, using data from 229 data pairs in California, South Carolina and Japan (72 are of Holocene age, 113 of Pleistocene age, and 44 of Tertiary age). Variables considered in the development of the equations include: corrected cone tip resistance (q_t), sleeve friction (f_s), depth (Z), soil behavior type index (I_C), overburden pressure, and geological age. Andrus et al. (2007) show that V_s generally increases with geological age for a given cone tip resistance.

Based on the Holocene data, the recommended best-fit equation for predicting V_s (m/s) is:

$$V_s = 2.27 \cdot q_t^{0.412} \cdot I_C^{0.989} \cdot Z^{0.033} \cdot ASF; ASF = 1 \tag{7}$$

where q_t is in kPa, I_C is dimensionless, Z is in m, and ASF is an age scaling factor with a value of 1.0 for Holocene soils.

Madiai and Simoni (2004) define regional empirical relationships between V_s, q_c and f_s and their data are collected from 22 cone penetration tests, 22 down-hole tests, and 2 cross-hole tests, with reference to two of the main formations present in the High Tiber Valley (Italy), namely: terraced and recent Holocene alluvium and

lacustrine and fluvio-lacustrine Pleistocene sediments. The correlations elaborated by Madiai and Simoni (2004) discriminate between fine-grained (cohesive) and coarse-grained soils (cohesionless), for each of the two formations, according to Robertson and Wride (1997) approach (soils with $I_C \leq 2.6$ are classified as non-cohesive, while soils with $I_C > 2.6$ are classified as cohesive).

The equations used in this paper are the following:

$$V_s = 140 \cdot {q_c}^{0.30} \cdot {f_s}^{-0.13} \quad \text{Holocene cohesive soils} \tag{8}$$

$$V_s = 268 \cdot {q_c}^{0.21} \cdot {f_s}^{0.02} \quad \text{Holocene non-cohesive soils} \tag{9}$$

where V_s is expressed in m/s, q_c and f_s in MPa.

4. Results

4.1 Bondeno site

The profiles of the geotechnical and geophysical parameters obtained at the Bondeno site are provided in Fig. 4a from the SCPTu and in Fig. 4b from the Medusa SDMT. In particular both *in situ* tests investigate the upper 20 m below the ground surface, providing the measurement of: the soil behavior type index (I_C), the corrected cone resistance (q_t), the sleeve friction (f_s) and the shear wave velocity (V_s) for the SCPTu, and the material index (I_D), the horizontal stress index (K_D), the constrained modulus (M_{DMT}) and the shear wave velocity (V_s) for the Medusa SDMT. The ground water table (GWT) was detected at 1 m depth in both soundings.

The I_C profile classifies the soil deposits mainly as silty clays in the first 4 m of depth, followed by sands, with a few lenses of silts and silty sands or sandy silts, down to the final SCPTu depth. The upper 4 m-crust is probably related to the fine sedimentary contribution of the Panaro river, followed by sands deposited by the Po River (Minarelli et al., 2022). The q_t and f_s profiles also identify a different behavior along the whole depth. The cone resistance is initially very low (below 2 MPa) while the sleeve friction presents a maximum (reaching 54 kPa at 2 m), as they do typically in cohesive layers. Then, the q_t measurements start to increase with depth, detecting a first sandy layer characterized by $q_t \approx$ 4-5 MPa between 4 and 7 m depth, and a second thicker and more uniform sandy layer with $q_t \approx$ 10-15 MPa from 7 to 19 m depth. The f_s values increase with depth, but are typically below 50 kPa, showing the presence of sands ($I_C \approx$ 1.5-2.0). The last panel of Fig. 4a shows three different V_s profiles measured with the SCPTu equipment using both the true-interval (T.I., average of left and right shots) and the pseudo-interval (P.I., lower and upper geophones) approaches. The pseudo-interval results generally gives lower values than the true-interval method, along the whole depth, with V_s values steadily increasing with depth from 130 m/s to roughly 230 m/s.

Looking at the results of the Medusa SDMT testing (Fig. 4b), the trend of the material index indicates the presence of fine-grained soils in the first 4 m, but instead of silty clays, as the soil behavior type index suggests, the I_D profile detects silts, clayey silts and sandy silts. Below 4 m depth, the soil deposits are identified mostly as silty sands and sandy silts, with $I_D \approx 1.8$. Although both I_C-SCPTu and I_D-Medusa SDMT usually detect the mechanical behavior and not the grain-size of the soil deposits, the different classification provided by the two *in situ* tests at the same study site may be related to the "intermediate" behavior of the silty deposits that have been already detected in other area of the Emilia plain (Monaco et al., 2021). Figure 4b also highlights that the K_D and M_{DMT} profiles have very similar trends: they both increase below 4 m, particularly evident for the constrained modulus, and identifies the presence of the two sand layers previously detected by q_t from SCPTu. The last panel of Fig. 4b shows three different V_s profiles measured with Medusa SDMT using both the true-interval (T.I., average of left and right shots) and the pseudo-interval (P.I., lower and upper geophones) approaches. Both approaches highlight a decreasing trend of V_s from the surface to 6 m depth and then an increase of V_s with depth, with values never exceeding 200 m/s for the true-interval V_s profile. The pseudo-interval method provides values that vary over a greater range compared to the true-interval interpretation, from about 90 m/s at 6 m depth to 280 m/s at 4 m depth.

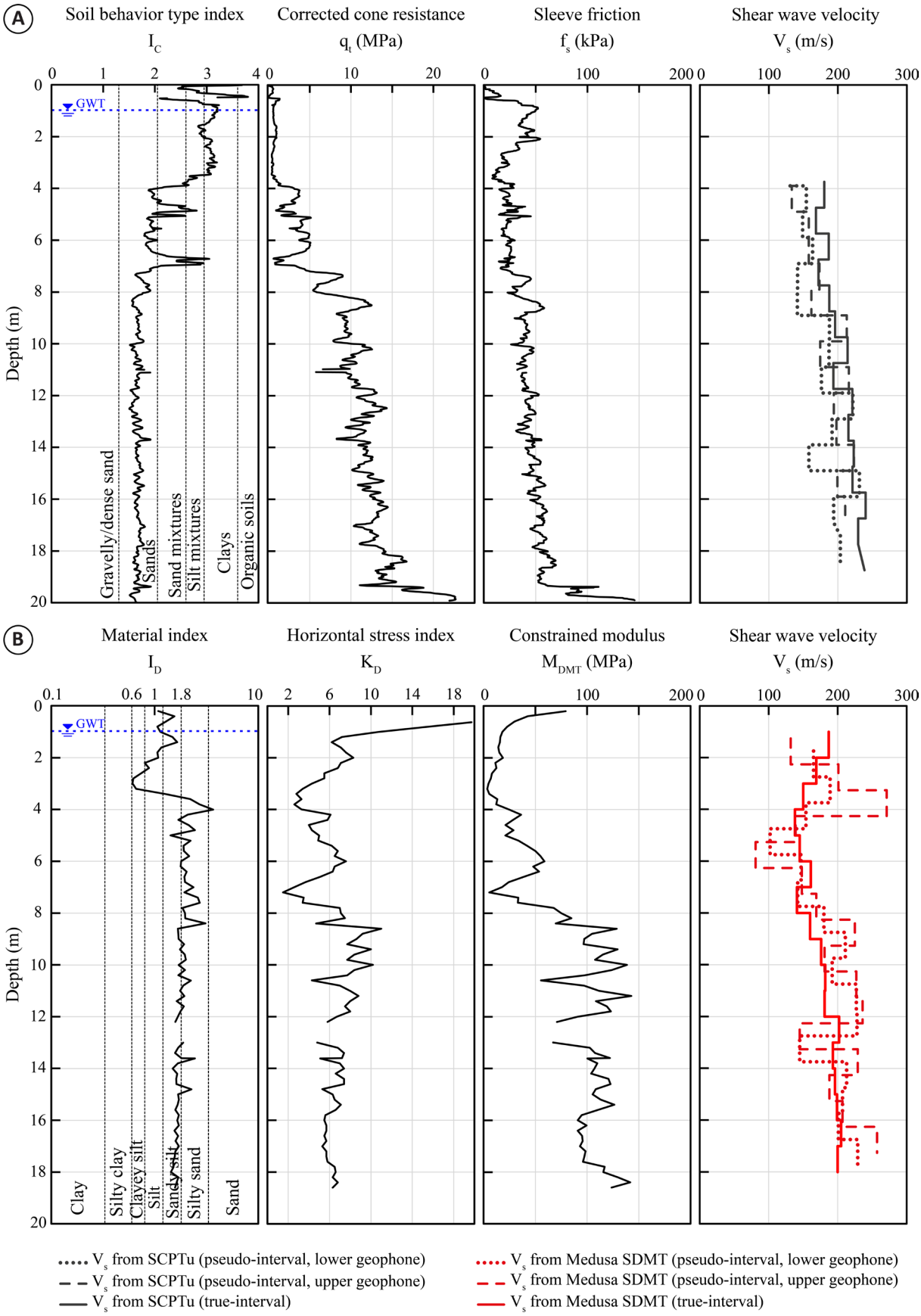

Figure 4. Measured parameters obtained with the SCPTu (a) and the Medusa SDMT (b) at the site of Bondeno.

4.2 Mirandola site

Figure 5 gives an overview at the geotechnical and geophysical characterization of the Mirandola site, considering the results obtained with the SCPTu (Fig. 5a) and with the Medusa SDMT (Fig. 5b). The ground water table is located at 1.7 m below the ground surface.

The I_C profile highlights mainly the presence of silty clays in the first 5 m of depth, which is also evident from the low values of cone resistance ($q_t < 2$ MPa). Below 5 m, both the I_C and q_t profiles detect the presence of sands with thin, fine interbedded layers, around 9.5 and 14.8 m. The upper 5 m-crust is probably related to the fine sedimentary contribution of the Secchia River, followed by sands deposited by the Po River (Minarelli et al., 2022). Four different sand layers can be identified based on the I_C, q_t and f_s profiles. The upper layer between 5 and 9.5 m, is characterized by q_t varying between 5 MPa and 10 MPa; while two sand layers characterized by a quite constant value of q_t, on average equal to 7 MPa (from 9.5 to 12 m) and 13 MPa (from 12 to 14.5 m); finally, another homogeneous sand layer from 14.5 to 19 m with $q_t \approx 8$ MPa. The sleeve friction is progressively decreasing in the first 6 m of depth, then it starts to increase, going up to 50 MPa between 12 and 15 m. The last panel of Fig. 5a illustrates three different V_s profiles measured with the SCPTu. It can be observed that there is better agreement between the true-interval and the pseudo-interval interpretations for Mirandola than for Bondeno, with V_s values steadily increasing with depth from about 100 m/s at 2 m depth to 280 m/s at 19 m depth.

Figure 5b completes the description of the Mirandola site with insights coming from the results of the Medusa SDMT testing. Below the upper 2 m-dry crust, the trend of the material index identifies the presence of silty clays up to 4-5 m, already detected by SCPTu, and of sandy silts between 5 and 18 m of depth, with I_D values varying within a very small range below 1.8. As already highlighted for the Bondeno site, the different soil classification provided by the SCPTu and Medusa SDMT at the Mirandola site for the silty-sandy layers may be related to the "intermediate" behavior of the soil deposits (Monaco et al., 2021). The different silty-sandy layers can be recognized also looking at the K_D and M_{DMT} profiles, with slightly different depth intervals in comparison with SCPTu: (from 5 to 8 m; from 8 to 12 m; from 12 to 14. 5 m; from 14.5 to 18 m). The horizontal stress index is lower than 6 between 2 and 5 m; then it is variable around the value of 6, reaching a maximum value of 10 at 7.8 and 13.2 m. Similarly, the constrained modulus provides very low values between 2 and 5 m ($M_{DMT} < 10$ MPa), and then very higher values (between 50 MPa and a maximum of 157 MPa at 13.2 m). Finally, the shear wave velocity profiles from the Medusa SDMT are shown; in this case, while for the pseudo-interval results the V_s values almost linearly increase with depth from 80 to 250 m/s, the true-interval results show V_s estimates varying in a close range around 200 m/s, excepting for a minimum around 120 m/s between 4 and 6 m depth.

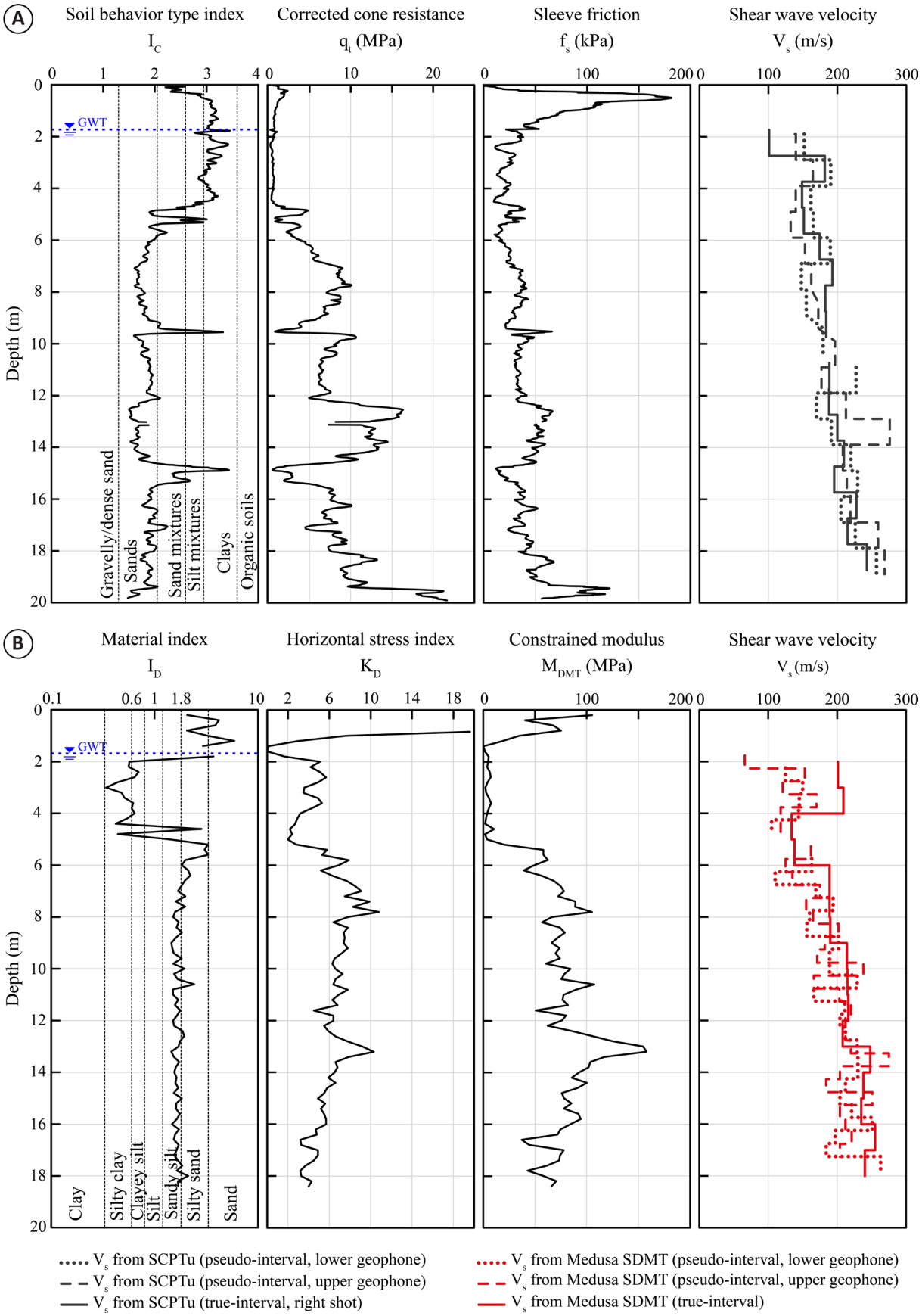

Figure 5. Measured parameters obtained with the SCPTu (a) and the Medusa SDMT (b) at the site of Mirandola.

4.3 Comparisons of V_S measured profiles

Figures 6a and 6b compare all the V_S measurements respectively at the Bondeno and Mirandola sites: three profiles from the SCPTu equipment, one true-interval (the average between the left shot and the right shot) and two pseudo-interval (relative to the upper and lower geophones) profiles, and equivalently for the Medusa SDMT test. Since the quality of acquired seismograms at shallow depths was not very good, they were removed from the SCPTu elaboration (at the Bondeno site the first V_S values are shown at 3.74 m).

Considering the V_S interpreted with the true-interval approach at the Bondeno site (Fig. 6a), the Medusa SDMT gives values that are always lower than the ones from SCPTu, while the use of the pseudo-interval method provides V_S profiles from Medusa SDMT and SCPTu fitting on average the true-interval profile from the Medusa SDMT.

In the case of Mirandola (Fig. 6b) we obtained a better agreement between the overall V_S values measured from the Medusa SDMT and the SCPTu tests. Referring to the true-interval approach, the Medusa SDMT gives generally higher V_S values than the SCPTu, while an opposite trend was identified at the Bondeno site. In general, the pseudo-interval method estimated V_S values with a significant scatter for the shallower layers ($Z < 4$ m). For larger depths, the pseudo-interval method applied to the SCPTu and SDMT data produced V_S profiles which are in better agreement than those produced by true-interval processing at each site.

The observed difference in the V_S profiles derived by pseudo-interval and true-interval approaches cannot be ascribed to the potentially erroneous calculation of effective seismic wave-paths. In fact, both methods suffer from the same limitation: they assume linear wave-paths between source and receivers. This approximation may severely overestimate seismic wave velocities, particularly when a stiff layer with higher velocities is located beneath a soft layer (Kim et al., 2004). Therefore, considering that the obtained V_S profiles do not show a sudden velocity increase and that at each site the SCPTu and SDMT survey locations are closely spaced but not identical, we argue that larger differences between true-interval solutions at the Bondeno site are likely due to the subsurface variability. The differences in the velocity estimates obtained by the pseudo-interval method at shallower depths may likely be due to inaccurate picking.

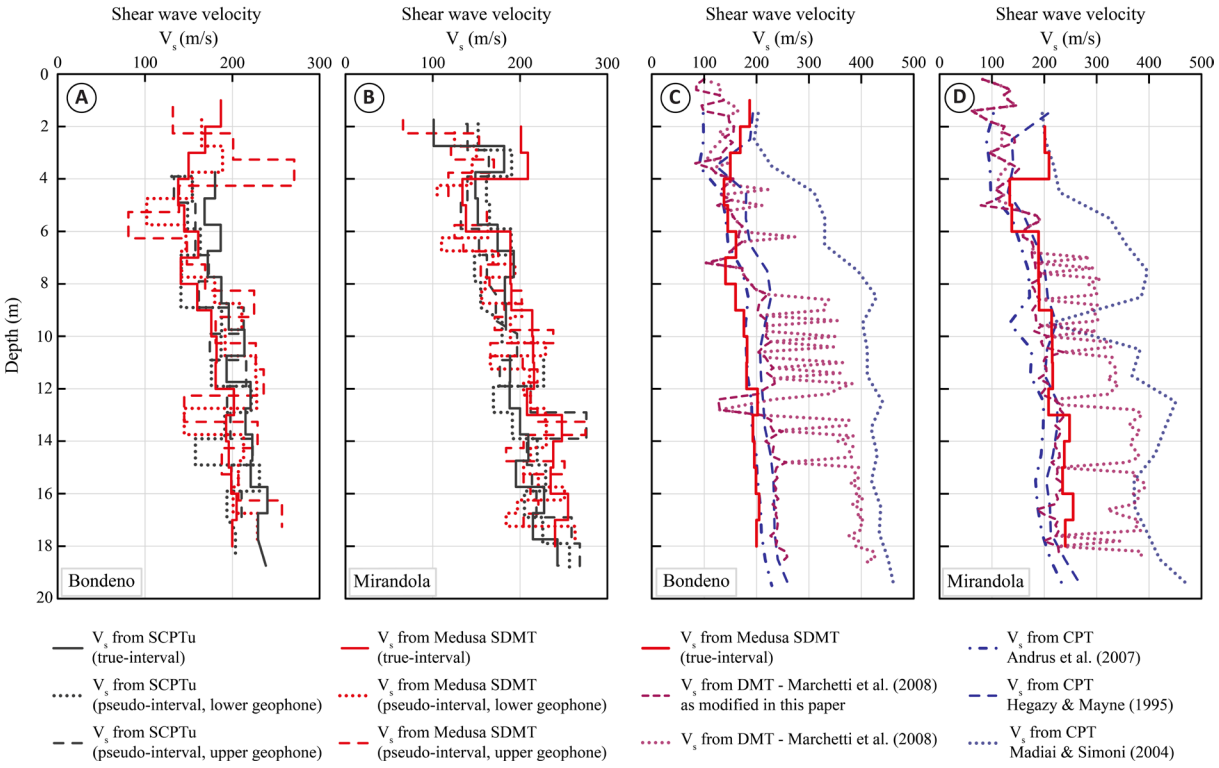

Figure 6. Comparisons of all the measured V_S profiles obtained from SCPTu and Medusa SDMT at Bondeno (a) and Mirandola (b) sites, using the pseudo-interval and true-interval approaches. Comparison of the Medusa SDMT V_S measurements obtained through the true-interval interpretation with the predicted V_S values estimated using CPT and DMT empirical correlations.

4.4 Comparisons of V_s estimated profiles

Figures 6c and 6d overlay the predicted V_s profiles estimated from the above introduced empirical DMT and CPT correlations with the V_s profiles measured from the Medusa SDMT using the true-interval interpretation. The results from this last approach are selected as reference because they are less prone to picking errors.

Two different V_s profiles were provided using the Marchetti et al. (2008) equations: one, named Marchetti et al. (2008), that considers the original predictive equations associated with the original ranges of the material index (i.e. Eq. (2) valid for clay characterized by $I_D \leq 0.6$; Eq. (3) valid for silts identified by $0.6 < I_D \leq 1.8$; Eq. (4) valid for sands associated to $I_D > 1.8$), and one, named Marchetti et al. (2008) modified, that refers to the original Marchetti et al. (2008) empirical correlations but restraining the limits of I_D for silts from 0.8 to 1.2, in relation to the possible "intermediate" behavior of these soil deposits. The equations adopted are the following:

$$\frac{G_0}{M_{DMT}} = 26.177 \cdot K_D^{-1.0066} \qquad Clays: I_D \leq 0.8 \tag{10}$$

$$\frac{G_0}{M_{DMT}} = 15.686 \cdot K_D^{-0.921} \qquad Silts: 0.8 < I_D \leq 1.2 \tag{11}$$

$$\frac{G_0}{M_{DMT}} = 4.5613 \cdot K_D^{-0.7967} \qquad Sands: I_D > 1.2 \tag{12}$$

The adjustments involved in the modified Marchetti et al. (2008) approach are suggested to produce better performance of the empirical correlations that estimate V_s and they are not related to DMT interpretation.

The V_s profiles estimated from the original Marchetti et al. (2008) model at Bondeno and Mirandola sites are extremely dependent on the soil type (I_D), resulting in significant overestimation of V_s in the silty deposits ($0.6 < I_D \leq 1.8$) but a small overestimation or in agreement with the measured V_s profile at depths where sand ($I_D > 1.8$) is found. As indicated in Figs. 4b and 5b, the I_D range between 0.6 and 1.8 includes also the soil layers classified as clayey silt and sandy silt, where a great part of the I_D data points of both Bondeno and Mirandola sites exists. To reduce the overestimation and to improve the performance of the DMT predictive model in these "intermediate" soils of the Emilia plain, this study suggests the modified I_D range of the original Marchetti et al. (2008) empirical correlations. Recently, Uzielli et al. (2024) also underlined the dependency of the original Marchetti et al. (2008) correlations from the soil type I_D, indicating that Eq. (2) significantly overestimates V_s for cohesive-behavior soils (clay), and Eq. (3) more appropriate for intermediate-behavior soils (silt).

With reference to the CPT predictive equations, Figs. 6c and 6d show significant overestimation of V_s values using the Madiai and Simoni (2004) empirical correlations, while the Hegazy and Mayne (1995) and Andrus et al. (2007) models agree quite well with the V_s measurements. In particular, the Hegazy and Mayne (1995) correlation provides a better agreement at the Mirandola site, while the Andrus et al. (2007) works better at the Bondeno site. As already noted by Zhou et al. (2023), the correlations based on CPT data tend to underestimate the measurements for low cone tip resistance and sleeve friction values (i.e. fine-grained soils), while at higher values (i.e. coarse-grained soils), they provide more reasonable estimates or overestimates.

The comparison of the CPT and DMT predictive models with the V_s measurements generally show a better performance of DMT than CPT, after the suggested modification is applied to the Marchetti et al. (2008) correlation. Previous studies, such as Marchetti (2010), Monaco et al. (2013), Amoroso (2014), Intriago et al. (2020) suggested that the V_s prediction from DMT, based on I_D, K_D and M_{DMT}, can provide more reliable and consistent results than the V_s estimation from CPT, presumably because of the DMT increased sensitivity to the stress history through K_D. This sensitivity is generally lost by the CPT since the cone destroys a large part of the soil structure during the penetration (large strain measurements), while it is more preserved by the lower strain penetration of the DMT wedge.

Finally, Fig. 7 plots the measured V_s values versus the estimated V_s values from the CPT and DMT V_s correlations at the same depths for the Bondeno and Mirandola sites. The black continuous line represents the perfect agreement:

Table 1. Values of RMSE (Root Mean Square Error) for each empirical correlation adopted in this work, calculated for both Bondeno and Mirandola sites (Eq. 13).

Empirical correlation	RMSE (m/s)	
	Bondeno	Mirandola
Hegazy & Mayne (1995)	37.1	30.7
Andrus et al. (2007)	32	56.9
Madiai & Simoni (2004)	204.9	154.9
Marchetti et al. (2008)	113.1	82.7
Marchetti et al. (2008) modified	37.3	31.2

each data point on that line indicates that the estimated V_s value is the same as the measured one at the same depth. If the data point falls below that line, it means that the empirical correlation provides an overestimation of the measured V_s value, while a data point above the same line, suggests an underestimation of the measured V_s. Each graph also includes two different dashed lines: the upper one is related to estimated values of V_s that are half of the corresponding measured values (0.5X), while the lower one is related to estimated values that are twice the corresponding measured ones (2X).

For each empirical correlation adopted at both the Bondeno and Mirandola sites, the Root Mean Square Error (RMSE, Eq. 13) is calculated and reported in Table 1, to provide a quantitative evaluation of the goodness-of-fit between measured and predictive models. The lower the RMSE, the better is the performance of the empirical correlation in estimating V_s from CPT or DMT data.

$$RMSE = \sqrt{\frac{\sum_{i=1}^{N}\left(V_{s,i\ measured} - V_{s,i\ estimated}\right)^2}{N}} \tag{13}$$

where $V_{s,i\ measured}$ and $V_{s,i\ estimated}$ are respectively the measured and estimated V_s (m/s) at the i-th acquisition depth and N is the number of acquisitions along the vertical profile.

Figures 7a and 7c clearly confirm the significant overestimation of the measured V_s value using the Madiai and Simoni (2004) results, since the predicted values are approximately double the measured V_s values (RMSE is 204.9 m/s at Bondeno site and 154.9 m/s at Mirandola site for this correlation). It is also clear that the Andrus et al. (2007) equation fits better at Bondeno site, while the Hegazy and Mayne (1995) method is better for the Mirandola site. The RMSE for Andrus et al. (2007) is 32 m/s at Bondeno site and 56.9 m/s at Mirandola site, while the RMSE for Hegazy and Mayne (1995) is 37.1 m/s at Bondeno site and 30.7 m/s at Mirandola site. Figures 7b and 7d clearly indicate the improvement in agreement between the measured and estimated V_s profiles obtained by adopting the modification of the Marchetti et al. (2008) method, suggested in this study. This improved agreement is valid at both the Bondeno and Mirandola sites, with many data points falling close to the continuous black lines, probably in relation to the "intermediate" behavior of these soil deposits. The RMSE for the original version of Marchetti et al. (2008) is 113.1 m/s at Bondeno site and 82.7 m/s at Mirandola site, while the application of the modified version proposed in this work brings the values of RMSE down to 37.3 m/s and 31.2 m/s, showing a significant reduction to values similar to those obtained with Hegazy and Mayne (1995) and Andrus et al. (2007).

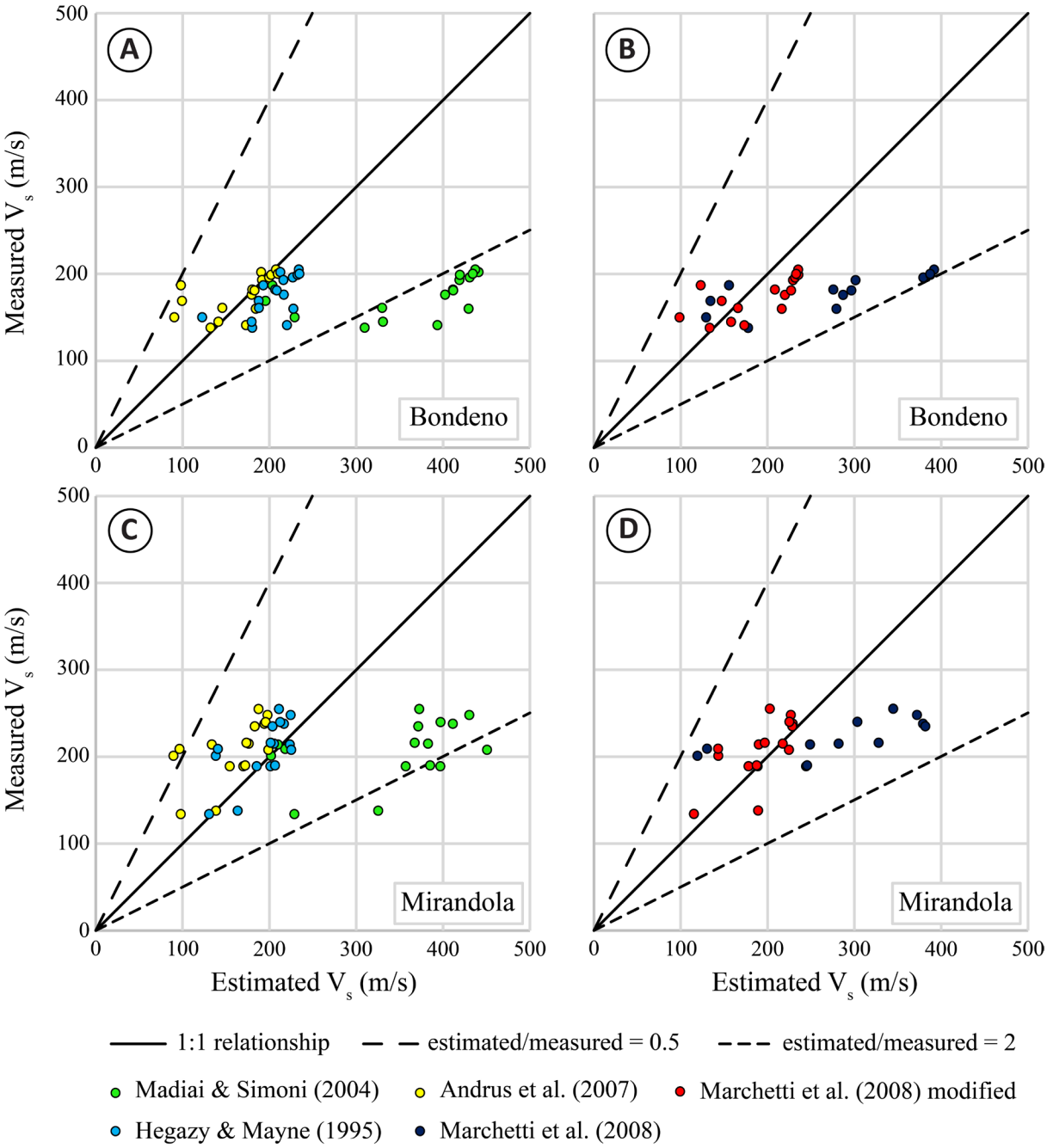

Figure 7. Comparison of the measured and estimated V_s at both Bondeno and Mirandola sites using existing CPT-V_s (a and c) and DMT-V_s (b and d) correlations. The lines represented in the figures indicate the matching between the V_s measurements and the predicted V_s values: if the points are aligned on the continuous line there is a perfect agreement; if the points are aligned on the upper dashed line the estimated values are half of the measured values; if the points are aligned on the lower dashed line the estimated values are twice the measured values.

4.5 Measured ratio G_0/M_{DMT} vs K_D compared with literature data (Marchetti et al., 2008)

Marchetti et al. (2008) remarks that G_0 is the small-strain shear modulus while M_{DMT} represents a working strain modulus corresponding to intermediate shear strains γ, ranging approximately between 0.01% and 2%, as indicated in Amoroso et al. (2014) and Di Mariano et al. (2019). The relationship between G_0 and M_{DMT} is interpreted in Marchetti et al. (2008) in terms of the normalized G/G_0-γ decay curve, where G is the shear modulus. These curves could be constructed by fitting "reference typical-shape" laboratory curves through two points: the initial modulus G_0 from V_s and a working strain shear modulus, G_{DMT}, obtained from M_{DMT} through the theory of linear elasticity,

valid in the intermediate shear strain range previously described. Marchetti et al. (2008) consider the shear modulus decay factor G_{DMT}/G_0 as a function of I_D and K_D finding that the shear modulus decay in sands is much greater than in silts and clays, which have a similar behavior. In addition, for all soils the decay is maximum for low K_D (NC or lightly OC soils). As it is also shown in Fig. 4b and Fig. 5b, the M_{DMT} is generally greater in sands rather than in clay and it grows with depth, since it depends on stress history. These combined observations lead to lower values of G_0/M_{DMT} in sand rather than in clay and silts with fixed K_D (it is in the range 0.5 to 3 in sand, 1 to 10 in silt, 1 to 20 in clay) and for all soils the ratio increases when K_D decreases. In conclusion, the ratio G_0/M_{DMT} is indicative of the stiffness decay factor and its variation with soil type and K_D reflects underlying mechanical behavior: the combined availability of G_0 and M_{DMT} provides two anchor points on the *in situ* G-γ curve.

The measured ratio G_0/M_{DMT}, expressed as a function of K_D and I_D are finally compared in Fig. 8 with the empirical correlations proposed by Marchetti et al. (2008) and already visible in Fig. 3. The data points are plotted considering the original I_D ranges (Figs. 8a and 8b) and considering the modified I_D ranges in which the silt is defined (Figs. 8c and 8d), associated to each equation (Eqs. (2), (3), (4)).

The measured values of G_0 from the Medusa SDMT (Eq. 5) are available each meter starting from 1.5 and 2.5 m depth at Bondeno and Mirandola sites, respectively. The constrained modulus, the horizontal stress index and the material index from the DMT are sampled every 20 cm depth. To couple the G_0 measured data points, the average M_{DMT} and K_D values are calculated, considering their values 10 cm above and 10 cm below the depths where G_0 is acquired. The ratios between G_0 and the average M_{DMT} values, corresponding at the same depth, are calculated and paired with the average K_D values: each data point ($G_0/M_{DMT} - K_D$) is classified in terms of I_D (as clay, silt or sand) to verify the agreement with literature trends. This classification is assigned taking into consideration the I_D values at both depths where DMT measured M_{DMT} and K_D were considered to obtain their average value. If they both fall within the same range of material index, the data point has an unequivocable classification (i.e. clay, silt or sand); if they fall in two different ranges, the classification is split between two soil classification (i.e. silt-sand, clay-sand, clay-silt).

Figures 8a and 8b illustrate how the data points are related to the trends of Marchetti et al. (2008), respectively referring to Bondeno and Mirandola sites. These two figures adopt the original ranges of I_D in which the three materials are classified and analyzing them, the agreement with the Marchetti et al. (2008) curves is not satisfactory, as many data points classified as silt or silt-sand fall along the sand curve. At the Mirandola site, two data points classified as silt and clay-silt fall far from the "clay" curve, while at the Bondeno site, two data points classified as silt fall perfectly along the "clay" curve. In addition, at both the sites many experimental data fall along the "sand" curve, although they are identified as silt and silt-sand.

Figures 8c and 8d show the same plots as Figs. 8a and 8b, adopting the modified I_D ranges suggested in this study for the Marchetti et al. (2008) equations. The data points change their classification because it is restrained the I_D interval in which silt is defined. These two figures allow to better understand how the modification improves the agreement with the literature trends: in both Bondeno (Fig. 8c) and Mirandola (Fig. 8d) sites, all the data points that fall along the "sand" curve are classified as sand. The improvement at Mirandola site is even better because the two data points that fall far from the "clay" curve become clay data points in Fig. 8d.

The quantitative evaluation of the improvement obtained in Figs. 8c and 8d is given by the calculation of RMSE with Eq. (14), whose values related to each panel of Fig. 8 as shown in Table 2. To take account of mixed data points, two different cases are depicted for each site. In each case, three different values of RMSE are obtained, one for each material considered (not every panel has all of them). The lower is the RMSE, the best is the correlation of measured G_0/M_{DMT} with the literature trend of Marchetti et al. (2008) and, therefore, also the classification of the material.

$$RMSE = \sqrt{\frac{\sum_{i=1}^{N}\left(\left(\frac{G_0}{M_{DMT}}\right)_{predicted} - \left(\frac{G_0}{M_{DMT}}\right)_{measured}\right)^2}{N}} \tag{14}$$

In Eq. (14), $(G_0/M_{DMT})_{measured}$ is obtained with direct measurement of G_0 (based on V_s through Eq. 5) and M_{DMT}, while $(G_0/M_{DMT})_{predicted}$ is obtained with the formulas of Marchetti et al. (2008) (Eqs. (2), (3), (4)), fixing the measured K_D at the same depth as $(G_0/M_{DMT})_{measured}$.

Referring to Fig. 8a, in Case 1 mixed data points are considered as silt, while in Case 2 they are considered as sand. Case 1 in Fig. 8b indicates silt-sand and clay-sand points as sand and clay-silt as clay; Case 2 considers silt-sand and

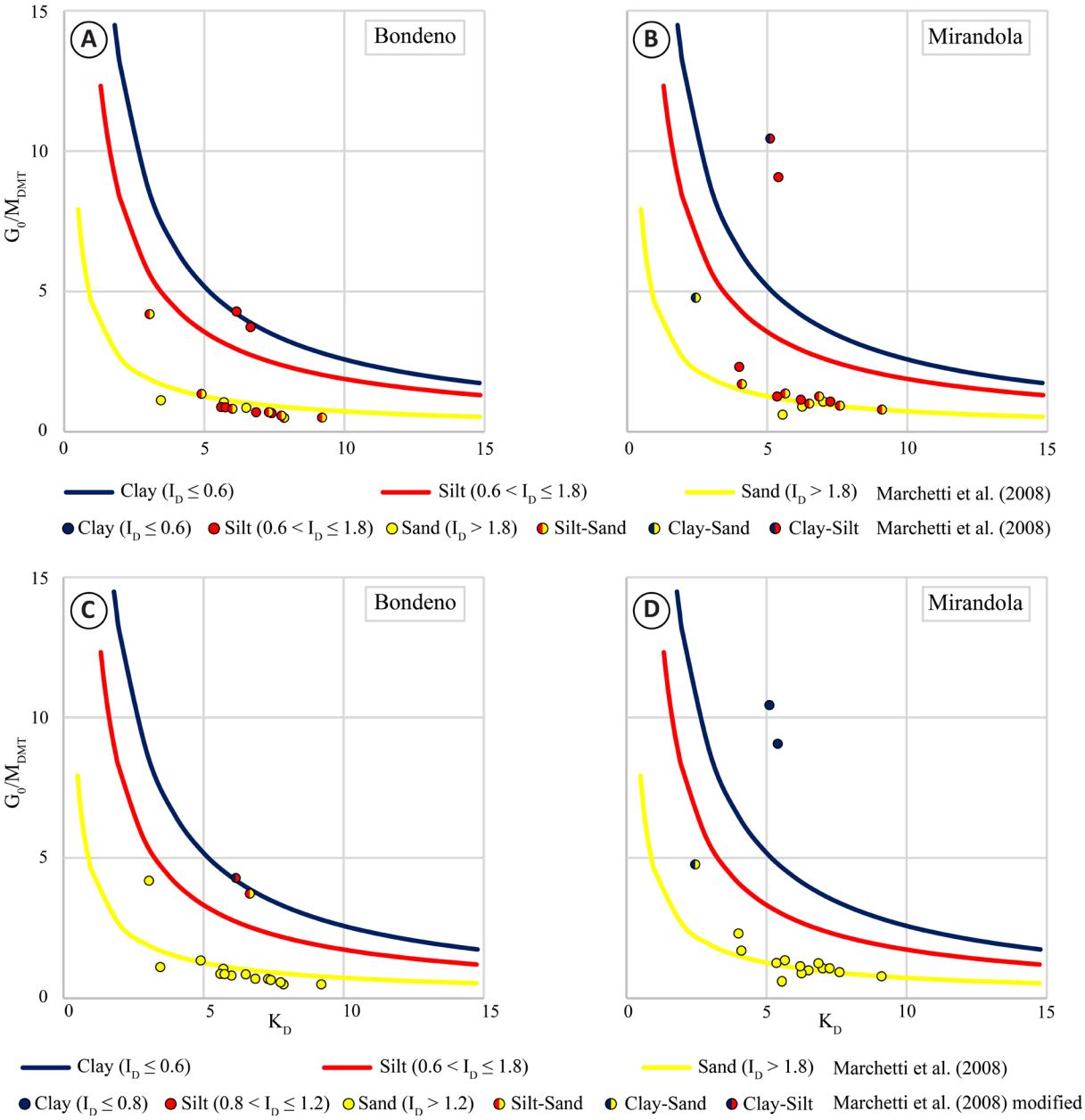

Figure 8. Comparison of the experimental ratio G_0/M_{DMT}, obtained respectively at the site of Bondeno (a) and Mirandola (b), using the Marchetti et al. (2008) correlation with the original I_D ranges. Comparison of the experimental ratio G_0/M_{DMT}, obtained respectively at the site of Bondeno (c) and Mirandola (d), using the Marchetti et al. (2008) correlation with the modified I_D ranges proposed in this study.

clay-silt points as silt and clay-sand as clay. Taking into consideration Fig. 8c, in Case 1 both mixed data points are considered as silt, while in Case 2 the silt-sand point is considered as sand and the clay-silt point is considered as clay. Finally, in the Case 1 of Fig. 8d the only mixed data point (clay-sand) is considered as clay and in Case 2 as sand.

The observation that can be stated analyzing Table 2 is that in both Case 1 and Case 2, when the comparison at the same site between RMSE values of a single material obtained with the original and the modified version of Marchetti et al. (2008) is available, there is always a reduction of RMSE, except for sand in Case 1 at Bondeno. In Case 1, RMSE goes from 1.9 to 1.2 for silt at Bondeno and it goes from 0.9 to 0.3 for sand and from 5.4 to 5.2 for clay at Mirandola, while in Case 2, it goes from 1.34 to 0.99 for sand at Bondeno and it goes from 1.3 to 0.8 for sand and from 5.8 to 4.9 for clay at Mirandola. The only increase of RMSE is recorded in Case 1 for sand at Bondeno, where it goes from 0.4 to 0.7. This can be explained considering that the sand data point acquired at 3.5 m depth in Fig. 8c is an outlier, given that its position is totally different from those of the other sand data points present

Table 2. Values of RMSE (Root Mean Square Error) for each site, adopting both the original and the proposed modified version of Marchetti et al. (2008). In order to take account of mixed data points, two different cases are depicted for each site (Eq. 14).

Site (approach)	RMSE (–) (Case 1)			RMSE (–) (Case 2)		
	Silt	Sand	Clay	Silt	Sand	Clay
Bondeno (Marchetti et al., 2008)	1.9	0.4	–	1.8	1.3	–
Bondeno (Marchetti et al., 2008 modified)	1.2	0.7	–	–	1	0.1
Mirandola (Marchetti et al., 2008)	3	0.9	5.4	3.1	1.3	5.8
Mirandola (Marchetti et al., 2008 modified)	–	0.3	5.2	–	0.8	4.9

in the same figure. If this point is not considered in the evaluation of RMSE, it varies from 0.4 to 0.3 for sand at Bondeno in Case 1, showing also in this case a reduction.

The distribution of many data points, classified as silt according to the I_D range in Figs. 8a and 8b but around the "sand" G_0/M_{DMT}-K_D curve, could be explained with reference to the transitional behavior of this kind of soil deposits. This discrepancy is highlighted also by the comparison of the measured V_s from Medusa SDMT (true interval) and the estimated V_s from Marchetti et al. (2008) in Figs. 6c and 6d. This kind of soils could be defined as "intermediate" and they include silts, silty sands, sandy silts and other soil mixtures. These soil types are typically present both at the Bondeno and Mirandola sites (see I_D profiles in Figs. 4b and 5b). Due to the variability of their main properties, the experimental behavior of these soils is still relatively poorly understood, and their characterization is a challenging issue, due to difficulties in undisturbed sampling, testing and interpretation of both laboratory and *in situ* experimental data (e.g. Schnaid et al., 2004; Schnaid et al., 2016).

These soils are considered as partially drained and their draining conditions could vary during penetration: their behavior and *in situ* partial drainage effects have already been thoroughly described in previous studies near Bondeno (Monaco et al., 2021) and in Norway (Monaco et al., 2024). Both these two papers remark that the penetration and pressurization rates during the Medusa DMT testing have a great influence on the response of intermediate soils in terms of drainage. In this respect, A and B measurements were acquired not only at standard penetration rate (20 mm/s) and at standard pressurization rate (15 s), but also at low (2 mm/s and 30 s) and at high (60 to 86 mm/s and 7.5 s) values of the penetration and pressurization rates. Low values of the penetration and pressurization rate lead to more drained conditions, moving I_D to the right towards the sand range. Penetration and pressurization rates higher than the standard rates make the conditions of the site more "undrained", moving I_D to the left towards the clay range. This behavior easily describes how the test conditions highly affect the results of the site characterization with Medusa DMT. This work shows the significant improvement provided by the adoption of the modified Marchetti et al. (2008) empirical correlations in intermediate soils, instead of the original versions, but a more rigorous demonstration of their efficiency for a larger database of geotechnical *in situ* tests results is needed.

5. Conclusions

The use of shear wave velocity for soil characterization is a critical aspect of geotechnical earthquake engineering: *in situ* tests are nowadays accompanied by many empirical correlations that predict the V_s profiles starting from the results of non-seismic tests such as SPT, CPT and DMT. These predictions may not be as accurate and reliable as the *in situ* direct V_s measurements, because they are strictly dependent on geotechnical and geophysical site characteristics. As a consequence, their applicability is often limited to the area in which the database of non-seismic

test has been developed. This paper has described the results of the SCPTu and Medusa SDMT testing held in two different sites in Emilia (Italy) in 2023.

The V_s profiles directly obtained with the two different *in situ* tests were elaborated adopting two different interval methods, the true-interval and the pseudo-interval approaches. The difference between the V_s results provided by the two approaches can be related to the different accuracy of the interpretation methods according to Garofalo et al. (2016) and Amoroso et al. (2016). The true-interval method is better conditioned since it is based on a wider portion of the seismograms, and not just on their first arrival, reducing the sensitivity to measurement errors, more typical of the pseudo-interval approach. Moreover, the differences in the velocity estimates obtained by the pseudo-interval method at shallower depths may be likely due to inaccurate picking. Both the adopted interval methods assume linear seismic wave-paths between source and receivers, even if Kim et al. (2004) remarks the importance of taking into consideration the effective seismic wave-paths to elaborate realistic V_s profiles. Given this observation, we can argue that larger differences between true-interval solutions at Bondeno are due to the surface variability and not to considering linear wave-paths.

The profiles obtained with the true-interval method Medusa SDMT were then chosen for the comparison of measured and CPT- and DMT-estimated values of V_s. This comparison shows a marked variability between profiles and it indicates limitations in the adopted correlations.

For CPT the Madiai and Simoni (2004) empirical model significantly overestimated the measured values, while Hegazy and Mayne (1995) and Andrus et al. (2007) correlations seem to give better performance with lower overestimations or underestimations.

For DMT the Marchetti et al. (2008) equations give back a peculiar trend of estimated V_s at both Bondeno and Mirandola site. This trend could be explained knowing that the materials investigated at both sites are intermediate soils. Intermediate soils typically exhibit partially drained behavior, that shifts to more drained or less drained conditions as a consequence of the testing procedures. This may lead to a misinterpretation of the nature of these soils, such as the definition as silts as materials that are instead closer to a sandy behavior. In this respect, this paper suggests a modification to the I_D ranges associated with the original Marchetti et al. (2008) relationship to improve its performance in predicting V_s in the Emilia plain. Specifically, the range of I_D values in which silt is defined according to Marchetti et al. (2008) is reduced, passing from $0.6 < I_D \leq 1.8$ to $0.8 < I_D \leq 1.2$. This modification showed improved performance of the DMT based empirical correlations but it should also be tested at other sites and larger databases, in order to be considered really useful at sites where intermediate soils predominate. Overall, these results demonstrate the value of further in-depth studies using variable-rate DMT and CPTu to improve the knowledge of soil characterization of intermediate soils.

Acknowledgements. Funding for this study was provided by a grant from the U.S. Geological Survey Earthquake Hazard Program under Grant No. G22AP00209-01. This support is gratefully acknowledged. However, the conclusions, opinions, and recommendations from this study are not necessarily those of the sponsors. We gratefully acknowledge Studio Prof. Marchetti S.r.l. (Italy) that kindly granted us the use of the Medusa SDMT during our *in situ* geotechnical test campaign in Emilia-Romagna and the SDMT Pro software. We also recognize the helpful concession of Pagani Geotechnical Equipment S.r.l. (Italy) in assisting us during the site campaign and of Geologismiki (Greece) in supplying us the free license of their software SPAS. Finally, we thank all the people who participated in the site investigation: Jonah Dundas (Brigham Young University, Utah), Gabriele Tarabusi and Stefano Maraio (Istituto Nazionale di Geofisica e Vulcanologia, Italy), Francesco Di Buccio (University of Chieti-Pescara, Italy) and Paolo Galloni (Pagani Geotechnical Equipment S.r.l., Italy).

References

Akin, M. K., S. L. Kramer and T. Topal (2011). Empirical correlations of shear wave velocity (V_s) and penetration resistance (SPT-N) for different soils in an earthquake-prone area (Erbaa-Turkey), Eng. Geol. 119, 1-17, doi:10.1016/j.enggeo.2011.01.007.

Amoroso, S. (2014). Prediction of the shear wave velocity V_s from CPT and DMT at research sites, Front. Struct. Civ. Eng., 8, 83-92, doi:10.1007/s11709-013-0234-6.

Amoroso, S., P. Monaco, B. Lehane and D. Marchetti (2014). Examination of the potential of the seismic dilatometer (SDMT) to estimate *in situ* stiffness decay curves in various soil types, Brazilian Association for Soil Mechanics

and Geotechnical Engineering (ABMS) and Portuguese Geotechnical Society (SPG), São Paulo, Brazil, Soils Rocks, 37, 3, 177-194, doi:10.28927/SR.373177.

Amoroso, S., C. Comina, S. Foti and D. Marchetti (2016). Preliminary results of P-wave and S-wave measurements by seismic dilatometer test (SPDMT) in Mirandola (Italy), Proceedings of the 5th International Conference on Geotechnical and Geophysical Site Characterization (ISC'5), Gold Coast, Queensland, Australia, September 5-19, 2016, Australian Geomechanics Society, 2, 825-830, ISBN:978-0-9946261-2-7.

Amoroso, S., G. Milana, K. M. Rollins, C. Comina et al. (2017). The first Italian blast-induced liquefaction test (Mirabello, Emilia-Romagna, Italy): description of the experiment and preliminary results, Ann. Geophys., 60, 5, S0556, doi:10.4401/ag-7415.

Amoroso, S., K. M. Rollins, P. Andersen, G. Gottardi et al. (2020). Blast-induced liquefaction in silty sands for full-scale testing of ground improvement methods: insights from a multidisciplinary study, Eng. Geol., 265, 105437, doi:10.1016/j.enggeo.2019.105437.

Andrus, R. D., N. P. Mohanan, P. Piratheepan, B. S. Ellis et al. (2007). Predicting shear-wave velocity from cone penetration resistance, Proc. 4th ICEGE, Thessaloniki, Greece.

ASTM D6635-01 (2017). Standard Test Method for Performing the Flat Plate Dilatometer, ASTM International, West Conshohocken, PA, USA.

ASTM D7400/D7400M-19 (2019). Standard Test Method for Downhole Seismic Testing, ASTM International, West Conshohocken, PA, USA.

ASTM D5778-12 (2020). Standard Test Method for Electronic Friction Cone and Piezocone Penetration Testing of Soil, ASTM International, West Conshohocken, PA, USA.

Baldi, G., R. Bellotti, V. N. Ghionna, M. Jamiolkowski et al. (1989). Modulus of sands from CPTs and DMTs, Proceeding of 12th International Conference on Soil Mechanics and Foundation Engineering, 1, Rio de Janeiro, 165-170.

Bellotti, R., M. Jamiolkowski, D. L. Lo Presti and D. A. O'Neill (1996). Anisotropy of small strain stiffness in Ticino sand, Geotechnique, 46, 1, 115-131, doi:10.1680/geot.1996.46.1.115.

Borchert, R. D. (1994). Estimates of site-dependent response spectra for design (methodology and justification), Earthq. Spectra, 10, 617-653, doi:10.1193/1.1585791.

Bouchovalas, G., N. Kalteziotis, N. Sabatakakis and C. Zervogiannis (1989). Shear wave velocity in a very soft clay-measurements and correlations, Proceedings of the 12th International Conference Soil Mechanics Foundation Engineering (ICSMFE), Rio de Janeiro, Brazil, 191-194.

Bruno, L., A. Amorosi, S. Lugli, I. Sammartino et al. (2021). Trunk river and tributary interactions recorded in the Pleistocene-Holocene stratigraphy of the Po Plain (northern Italy), Sedimentology, 68, 2918-2943, doi:10.1111/sed.12880.

Campanella, R. G., P. K. Robertson and D. Gillespie (1986). Seismic cone penetration test, Use of *In situ* Tests in Geotechnical Engineering, GSP 6, ASCE, Reston/VA, 116-130.

Campanella, R. G. (1994). Field methods for dynamic geotechnical testing: an overview of capabilities and needs, in Dynamic Geotechnical Testing II (STP 1213), ASTM International, R. J. Ebelhar, V. P. Drnevich and B. L. Kutter (Eds.), 100 Barr Harbor Drive, PO Box C700, West Conshohocken/PA, 3-23, doi:10.1520/STP13203S.

CEN, Comité Européen de Normalisation (2004). Eurocode 8: Design of structures for earthquake resistance – Part 1: General rules, seismic actions and rules for buildings, Brussels, Belgium.

Civico, R., C. A. Brunori, P. M. De Martini, S. Pucci et al. (2015). Liquefaction susceptibility assessment in fluvial plains using airborne LIDAR: the case of the 2012 Emilia earthquake sequence area (Italy), Nat. Hazards Earth Syst. Sci., 15, 2473-2483, doi:10.5194/nhess-15-2473-2015.

Demurtas, L., D. Fontana, S. Lugli and L. Bruno (2024). Multi-source detrital contributions in the Po alluvial basin (northern Italy) since the Middle Pleistocene. Insights into sediment accumulation in intermediate sinks, Basin Res., 36, e12858, doi:10.1111/bre.12858.

Di Mariano, A., S. Amoroso, M. Arroyo, P. Monaco et al. (2019). Case Study: SDMT-based numerical analyses of a deep excavation in soft soil, J. Geotech. Geoenviron. Eng. ASCE, 145, 1, 04018102, 12, doi:10.1061/(ASCE) GT.1943-5606.0001993.

Fear, C. E. and P. K. Robertson (1995). Estimating the undrained strength of sand: a theoretical framework, Can. Geotech. J., 32, 5, 859-870, doi:10.1139/t95-082.

Facciorusso, J., C. Madiai and G. Vannucchi (2015). CPT-based liquefaction case history from the 2012 Emilia earthquake in Italy, J. Geotech. Geoenviron. Eng. ASCE, 141, 12, 1032-1051, doi:10.1061/(ASCE)GT.1943-5606.0001349.

Flora, A., E. Bilotta, A. Chiaradonna, S. Lirer et al. (2021). A field trial to test the efficiency of induced partial saturation and horizontal drains to mitigate the susceptibility of soils to liquefaction, Bull. Earthq. Eng.,19, 10, 3835-3864, doi:10.1007/s10518-020-00914-z.

Garofalo, F., S. Foti, F. Hollender, P. Y. Bard et al. (2016). InterPACIFIC project: Comparison of invasive and non-invasive methods for seismic site characterization. Part II: Inter-comparison between surface-wave and borehole methods, Soil Dyn. Earthq. Eng., 82, 241-254, doi:10.1016/j.soildyn.2015.12.009.

Hegazy, Y. A. and P. Mayne (1995). Statistical correlations between V_s and cone penetration data for different soil types, Proc. International Symposium on Cone Penetration Testing, CPT, Linkoping, Sweden, 173-178.

Hepton, P. (1988). Shear wave velocity measurements during penetration testing, Proc. Penetration Testing in the UK, ICE, 275-278.

Intriago, B., H. Bazurto, D. Besenzon, X. Vera-Grunauer et al. (2020). Shear wave velocity prediction using different *in situ* tests at a soft clayey site in Guayaquil (Ecuador), Proceedings of 6th International Conference on Geotechnical and Geophysical Site Characterization (ISC2020), doi:10.53243/ISC2020-522.

Jamiolkowski, M. and D. C. F. Lo Presti (1991). Anisotropy of Soil Stiffness at Small Strain, Panel Discussion to Session 1, 9th ARC on SMFE, Bangkok.

Jamiolkowski, M. and D. C. F. Lo Presti (1998). Geotechnical Characterization of Gravelly Deposits, 13th SEAGC, Taipei, Taiwan, 107-124.

Kim, D. S., E. S. Bang and W. C. Kim (2004). Evaluation of various downhole data reduction methods for obtaining reliable V_s profiles, Geotech. Test. J., 27, 6, 585-597, doi:10.1520/GTJ11811.

Lo Presti, D. C. F. and D. A. O'Neill (1991). Laboratory investigation of small strain modulus anisotropy in sands, Proceedings of the ISOCCTI, Clarkson University, Potsdam, 213-224.

Lo Presti, D., M. Jamiolkowski, A. Cavallaro and O. Pallara (1999). Anisotropy of small strain stiffness of undisturbed and reconstituted clays, Proceedings of Pre-failure Deformation Characteristics of Geomaterials, Balkema, 1, 3-10.

Lo Presti, D., F. Fiera, M. Perini, E. Pagani et al. (2024). Use of seismic piezocone for the assessment of the propagation velocity of body waves, Rivista Italiana di Geotecnica, Anno LVIII, 2, 90-98, doi:10.19199/2024.2.0557-1405.090.

Madiai, C. and G. Simoni (2004). Shear wave velocity-penetration resistance correlation for Holocene and Pleistocene soils of an area in central Italy, Proc. 2nd ISC'2, Porto, Portugal, 1687-1694.

Marchetti, D. (2018). Dilatometer and Seismic Dilatometer Testing Offshore: Available Experience and New Developments, Geotech. Test. J., 41, 5, 967-977, doi:10.1520/GTJ20170378.

Marchetti, S. (1980). *In situ* Tests by Flat Dilatometer, J. Geotech. Eng. Div., 106, 299-321.

Marchetti, S. and D. K. Crapps (1981). Flat dilatometer manual, Internal report of GPE.

Marchetti, S. (2010). Sensitivity of CPT and DMT to stress history and aging in sands for liquefaction assessment, Proceedings of the CPT 2010 International Symposium Huntington Beach, California.

Marchetti, S., P. Monaco, G. Totani and D. Marchetti (2008). *In situ* tests by seismic dilatometer (SDMT), Proceedings of from research to practice in geotechnical engineering, USA, New Orleans, 292-311, doi:10.1061/40962(325)7.

Marchetti, D., P. Monaco, S. Amoroso and L. Minarelli (2019). *In situ* tests by Medusa DMT, Proceedings of XVII ECSMGE Reykjavik, doi:10.32075/17ECSMGE-2019-0657.

Mayne, P. W. (2006). *In situ* test calibrations for evaluating soil parameters, Characterization and Engineering Properties of Natural Soils, 3, 1601-1652, doi:10.1201/NOE0415426916.ch2.

McGann, C. R., B. A. Bradley, M. L. Taylor, L. M. Wotherspoon et al. (2015). Development of an empirical correlation for predicting shear wave velocity of Christchurch soils from cone penetration test data, Soil Dyn. Earthq. Eng., 75, 66-75, doi:10.1016/j.soildyn.2015.03.023.

Minarelli, L., S. Amoroso, R. Civico, P. M. De Martini et al. (2022). Liquefied sites of the 2012 Emilia earthquake: a comprehensive database of the geological and geotechnical features (Quaternary alluvial Po plain, Italy), Bull. Earthq. Eng., 20, 3659-3697, doi:10.1007/s10518-022-01338-7.

Monaco, P., S. Amoroso, S. Marchetti, D. Marchetti et al. (2013). Overconsolidation and stiffness of Venice Lagoon sands and silts from SDMT and CPTU, J. Geotech. Geoenviron. Eng., 140, 1, 215-227, doi:10.1061/(ASCE)GT.1943-5606.0000965.

Monaco, P., L. Tonni, S. Amoroso, M. F. Martinez et al. (2021). Use of Medusa DMT in alluvial silty sediments of the Po River valley, Proceeding of 6th International Conference on Geotechnical and Geophysical Site Characterization (ISC2020), Budapest, Hungary, doi:10.53243/ISC2020-424.

Monaco, P., S. Amoroso, A. Chiaradonna, D. Marchetti et al. (2024). Characterization of intermediate soils by innovative *in situ* testing procedures using Medusa DMT, Proceedings of the XVIII European Conference on soil mechanics and geotechnical engineering, doi:10.1201/9781003431749-109.

Pondrelli, S., S. Salimbeni, P. Perfetti and P. Danecek (2012). Quick regional centroid moment tensor solutions for the Emilia 2012 (northern Italy) seismic sequence, Ann. Geophys., 55, 4, 615-621, doi:10.4401/ag-6146.

Reynolds, J. M. (1997). An Introduction to Applied and Environmental Geophysics, J. Wiley and Sons, New York, 712, ISBN:978-0-471-485360.

Rix, G. J. and K. H. Stokoe (1991). Correlation of initial tangent modulus and cone penetration resistance, Proceedings Calibration Chamber Testing, ISOCCT-1, Elsevier Publishing, New York, 351-362.

Robertson, P. K., R. G. Campanella, D. Gillespie and J. Greig (1986) Use of piezometer cone data, Use of *In situ* Testing in Geotechnical Engineering, GSP, 6, ASCE, Reston/VA, 1263-1280.

Robertson, P. K. (2009). Interpretation of cone penetration tests – a unified approach, Can. Geotech. J., 46, 11, 1337-1355, doi:10.1139/T09-065.

Robertson, P. K. and C. E. Wride (1997). Cyclic liquefaction and its evaluation based on the SPT and CPT, Proceedings of the National Center for Earthquake Engineering Research (NCEER) Workshop on Evaluation of Liquefaction Resistance of Soils, Salt Lake City, Utah, January 5-6, 1996 Technical Report NCEER-97-0022, 41-87.

Roesler, S. K. (1979). Anisotropic shear modulus due to stress anisotropy, J. Geotech. Eng. Div., 105, 7, 871-880, doi:10.1061/AJGEB6.0000835.

Schnaid, F., B. M. Lehane and M. Fahey (2004). *In situ* test characterization of unusual geomaterials, Proceedings of the 2nd International Conference on Site Characterization ISC-2, Porto, Portugal, 1, 49-73.

Schnaid, F., E. Odebrecht, J. Sosnoski and P. K. Robertson (2016). Effects of test procedure on flat dilatometer test (DMT) results in intermediate soils, Can. Geotech. J., 53, 8, 1270-1280, doi:10.1139/cgj-2015-0463.

Simonini, P. and S. Cola (2000). Use of piezocone to predict maximum stiffness of Venetian soils, J. Geotech. Geoenviron. Eng., 126, 4, 378-382, doi:10.1061/(ASCE)1090-0241(2000)126:4(378).

Stacul, S., F. Fiera, M. Perini, E. Pagani et al. (2024). On the assessment of compression and shear wave velocities via seismic cone penetration test and comparisons with other geophysical tests at different sites, J. GeoEngin, 19, 4, 160-168, doi:10.6310/jog.202412_19(4).4.

Stefani, S., L. Minarelli, A. Fontana and I. Hajdas (2018). Regional deformation of late Quaternary fluvial sediments in the Apennines foreland basin (Emilia, Italy), Int. J. Earth Sci., 107, 7, 2433-2447, doi:10.1007/s00531-018-1606-x.

Stokoe, K. H. II, J. N. K. Lee and S. H. H. Lee (1991). Characterization of soil in calibration chambers with seismic waves, Proceedings of the ISOCCTI, Clarkson University, Potsdam.

Tonni, L., G. Gottardi, S. Amoroso, R. Bardotti et al. (2015). Interpreting the deformation phenomena triggered by the 2012 Emilia seismic sequence on the Canale Diversivo di Burana banks. Rivista Italiana di Geotecnica, Anno XLIX, 2, 28-38, http://www.associazionegeotecnica.it/sites/default/files/rig/2_2015_028ton.pdf.

Uzielli, M., D. Marchetti and S. Amoroso (2024). Comparative assessment of DMT-based and CPT-based transformation models for the estimation of shear wave velocity: a case study in central Italy, Proceedings of the 7th International Conference on Geotechnical and Geophysical Site Characterization, Barcelona, Spain, 18-21 June 2024, doi:10.23967/isc.2024.146.

Vera-Grunauer, X. (2014). Seismic response of a soft, high plasticity, diatomaceous naturally cemented clay deposit, PhD thesis, University of California, Berkeley.

Woods, R. D. (1978). Measurement of dynamic soil properties, Soil Dyn. Earthq. Eng., I, ASCE Conference, Pasadena, 91-178.

Zhou, H., L. M. Wotherspoon, C. P. Hayden, A. C. Stolte et al. (2023). Applicability of existing CPT-Vs correlations to shallow Holocene Christchurch soils based on direct Push crosshole testing, Eng. Geol., 313, 106927, doi:10.1016/j.enggeo.2022.106927.

***CORRESPONDING AUTHOR: Christian VALVANO**,
University of Chieti-Pescara, Pescara, Italy
e-mail: christian.valvano@studenti.unich.it